HHS Public Access

Author manuscript

Clin Cancer Res. Author manuscript; available in PMC 2017 April 01.

Published in final edited form as:

Clin Cancer Res. 2016 April 1; 22(7): 1687–1698. doi:10.1158/1078-0432.CCR-14-3378.

Hypoxia-activated prodrug TH-302 targets hypoxic bone marrow niches in pre-clinical leukemia models

Juliana Benito[1], **Marc Ramirez**[2], **Niki Zacharias Millward**[3], **Juliana Velez**[1], **Karine Harutyunyan**[1], **Hongbo Lu**[1], **Yuexi Shi**[1,†], **Polina Matre**[1], **Rodrigo Jacamo**[1], **Helen Ma**[1], **Sergej Konoplev**[4], **Teresa McQueen**[1], **Andrei Volgin**[5], **Marina Protopopova**[6], **Hong Mu**[1], **Jaehyuk Lee**[2], **Pratip Bhattacharya**[7], **Joseph R Marszalek**[6], **R. Eric Davis**[8], **Jim Bankson**[2], **Jorge Cortes**[1], **Charles P Hart**[9], **Michael Andreeff**[1], and **Marina Konopleva**[1]

[1]Department of Leukemia, UT MD Anderson Cancer Center, Houston, Texas

[2]Imaging Physics, UT MD Anderson Cancer Center, Houston, Texas

[3]Department of Experimental Diagnostic Imaging, UT MD Anderson Cancer Center, Houston, Texas

[4]Department of Hematopathology, UT MD Anderson Cancer Center, Houston, Texas

[5]Department of Bioinformatics and Computational Biology, UT MD Anderson Cancer Center, Houston, Texas

[6]Institute for Applied Cancer Science, UT MD Anderson Cancer Center, Houston, Texas

[7]Cancer Systems Imaging, UT MD Anderson Cancer Center, Houston, Texas

[8]Department of Lymphoma and Myeloma, UT MD Anderson Cancer Center, Houston, Texas

[9]Threshold Pharmaceuticals, Inc., South San Francisco, California

Abstract

Corresponding Author: Marina Konopleva, MD, PhD, Department of Leukemia, The University of Texas MD Anderson Cancer Center, 1515 Holcombe Blvd., Unit 428, Houston, TX 77030, mkonople@mdanderson.org, Phone: (713) 563-6700.

†deceased

Author Contribution: Design and performed experiments, analyzed data, wrote and edited manuscript: J. Benito, M. Konopleva

Design and performed experiments, analyzed data, edited manuscript: M. Ramirez, N. Millward, R. Jacamo,

Performed experiments: H. Lu, Y. Shi, T. McQueen, H. Ma, M. Protopopova, H. Mu, J. Lee

Performed in vivo experiments: J. Velez

Conducted immunohistochemistry staining, assisted in writing the manuscript: K. Harutyunyan

Analyzed immunohistochemistry, assisted in writing the manuscript: S. Konoplev

Analyzed data, edited manuscript: P. Matre

Design and performed experiments, analyzed data: A. Volgin

Design experiments, analyzed data, edited manuscript: P. Bhattacharya, J. Marszalek, R. Davis, J. Bankson

Edited manuscript: J. Cortes, M. Andreeff

Design experiments, edited manuscript: C. Hart

Disclosure of Potential Conflicts of Interest: Charles Hart is employed by Threshold Pharmaceuticals the maker of TH-302. The study was partially funded by Threshold. All other authors declare no conflict of interest.

Purpose—to characterize the prevalence of hypoxia in the leukemic bone marrow (BM), its association with metabolic and transcriptional changes in the leukemic blasts and the utility of hypoxia activated prodrug TH-302 in leukemia models.

Experimental design—hyperpolarized magnetic resonance spectroscopy was utilized to interrogate the pyruvate metabolism of the bone marrow in the murine AML model. Nanostring technology was used to evaluate a gene set defining a hypoxia signature in leukemic blasts and normal donors. The efficacy of the hypoxia-activated pro-drug TH-302 was examined in the in vitro and in vivo leukemia models.

Results—Metabolic imaging has demonstrated increased glycolysis in the femur of leukemic mice compared to healthy control mice, suggesting metabolic re-programming of hypoxic BM niches. Primary leukemic blasts in samples from AML patients overexpressed genes defining a "hypoxia index" compared to samples from normal donors. TH-302 depleted hypoxic cells, prolonged survival of xenograft leukemia models and reduced the leukemia stem cell pool in vivo. In the aggressive FLT3/ITD MOLM-13 model, combination of TH-302 with tyrosine kinase inhibitor sorafenib had greater anti-leukemia effects than either drug alone. Importantly, residual leukemic BM cells in a syngeneic AML model remain hypoxic after chemotherapy. In turn, administration of TH-302 following chemotherapy treatment to mice with residual disease prolonged survival, suggesting that this approach may be suitable for eliminating chemotherapy-resistant leukemia cells.

Conclusions—These findings implicate a pathogenic role of hypoxia in leukemia maintenance and chemoresistance and demonstrate the feasibility of targeting hypoxic cells by hypoxia cytotoxins.

Keywords

TH-302; hypoxia; AML; bone marrow; cytotoxins

Introduction

Acute myeloid leukemia (AML) is a molecularly heterogeneous disease characterized by an expansion of immature blood cells due to impaired self-renewal, differentiation, and apoptosis. High relapse rates, thought to be due to persistence of chemoresistant leukemia cells, and refractoriness to second line chemotherapy remain major therapeutic challenges associated with poor outcomes(1). The leukemic microenvironment has been implicated in chemoresistance and nurturing of leukemia-initiating cells through multiple mechanisms(2). Recent findings from our group and others (3-5) demonstrated that hypoxia is a prevalent feature of the leukemic, but not the normal, BM microenvironment. Utilizing murine leukemia models, we showed vast expansion of hypoxia niches within the leukemic BM microenvironment that paralleled leukemia progression. Similarly, hypoxia was shown to be present in multiple myeloma *in vivo* models and to correlate with disease progression and aggressiveness(3, 4). Pathologic hypoxia is a common feature in many solid tumors and is associated with increased tumor aggressiveness and resistance to therapy, mediated at least in part through activation of hypoxia-inducible factor 1α (HIF-1α)(6-8). Indeed, in acute lymphoblastic leukemia (ALL) cells, pharmacologic or genetic stabilization of HIF-1α

under normoxic conditions inhibited cell growth and reduced apoptosis induction by chemotherapeutic agents, while inhibition of HIF-1α expression promoted chemosensitivity of ALL cells cultured under hypoxic conditions(9). Our previous data showed that HIF-1α protein was expressed in the BM biopsies of ∼60% of Philadelphia chromosome-negative B-ALL patients but was undetectable in normal donor BM, suggesting the importance of HIF-1α in the leukemic BM microenvironment(10). Matsunaga *et al.* reported that HIF-1α promotes quiescence of leukemic stem cells residing in the endosteal niches and suggested that this could contribute to minimal residual disease in AML(11).

HIF-1α induces the expression of an array of genes regulating angiogenesis, invasiveness, drug resistance and glycolysis(12, 13). Magnetic resonance spectroscopy (MRS) is an analytical technique that allows for non-radioactive isotopes (such as ^{1}H, ^{13}C, ^{31}P) to be detected in a high field magnet. Because nuclei in different chemical environments will have slightly different resonance frequencies, MRS can be used to determine the metabolic profile of biological samples *ex vivo* or *in vivo*(14, 15). However, real time metabolic imaging is not possible with conventional MRS, which requires the averaging of multiple readings to generate a well resolved spectrum. This problem has been solved by a new method called hyperpolarized MRS, which achieves a >10,000 fold enhancement of signal over conventional MRS, allowing non-toxic and non-radioactive imaging of metabolic products after addition of a hyperpolarized agent to a biological system(16-18). Hyperpolarized (HP) ^{13}C-enriched pyruvate, a novel diagnostic substrate, has been utilized to interrogate glycolytic metabolism in leukemia bearing mice and normal controls *in vivo* through tracing the metabolism of pyruvate to alanine, lactate and bicarbonate(16-18). Under hypoxic conditions, cancer cells re-wire their metabolism by increasing glucose uptake and utilizing anaerobic glycolysis for energy generation. This increase leads to high levels of lactate production through pyruvate being utilized by lactate dehydrogenase. Using hyperpolarized pyruvate technology, the glycolytic flux of lactate dehydrogenase can be monitored in real time. The higher the flux rates, the greater use of glycolysis in that particular tissue.

Hypoxia-activated prodrugs (HAPs) are designed to deliver cytostatic or cytotoxic effects to hypoxic subregions. In most cases, the first step in their activation reaction consists of a one-electron reduction of the prodrug by generally ubiquitous one-electron reductases(19-21), resulting in a prodrug radical that undergoes redox cycling in the presence of oxygen(22). Under hypoxic conditions, the radical has a much longer lifetime and undergoes fragmentation or further reduction, leading to formation of the active drug in hypoxic cells. We have previously shown the effectiveness of HAP PR-104 in preclinical leukemia models, supporting the concept for the selective cytotoxic targeting of the hypoxic leukemic environment(23), and recently reported the results of the Phase I clinical trial.(24)

TH-302 is a HAP that is currently in clinical testing for a broad series of indications, including myeloma and AML/ALL. Upon reduction of a nitro group in TH-302, the prodrug releases a DNA-crosslinking mustard alkylating agent (bromo-isophosphoramide) in hypoxic regions(25, 26). In multiple myeloma models, TH-302 demonstrated profound *in vitro* and *in vivo* antitumor activity(27).

In this study, we characterized the leukemic microenvironment through hypoxia-regulated gene expression studies, dynamic MRS of HP-pyruvate *in vivo* and interrogation of residual hypoxic leukemia cells surviving chemotherapy using the hypoxia-activated prodrug TH-302. Our findings confirm the premise that hypoxia is a prominent component of leukemia and demonstrate the improved anti-leukemia efficacy of combining traditional therapeutics with hypoxia-targeting agents.

Materials and Methods

Chemicals, antibodies, and reagents

TH-302 was provided by Threshold Pharmaceuticals. Cytarabine, doxorubicin, 5-azacytidine, and decitabine were purchased from the pharmacy of The University of Texas MD Anderson Cancer Center. Sorafenib was acquired from Selleckchem. Fluorescein isothiocyanate–conjugated mouse monoclonal anti-pimonidazole (PIMO) antibody (Hypoxyprobe, Inc.) was used for immunohistochemical (IHC) analysis. Antibodies used for fluorescence-activated cell sorting (FACS) were AnnexinV-Cy5, mouse anti-human CD45, rat anti-mouse CD45, mouse anti-human CD34, and mouse anti-human CD123 (BD Biosciences). Propidium iodide (PI) and 7-amino-actinomycin D (7AAD) were purchased from Sigma Chemical.

Cell lines and human patient samples

KG-1, REH, and Nalm-6 cells were purchased from American Type Tissue Collection and MOLM-13 cells from DSMZ. KBM-5 and OCI-AML3 cells were kindly provided by Dr Miloslav Beran (M.D. Anderson Cancer Center, Department of Leukemia) and Dr Mark Minden (Princess Margaret Cancer Center, Toronto, Canada), respectively. All cell lines were tested and authenticated by STR DNA fingerprinting performed by the Characterized Cell Line Core facility at MD Anderson Cancer Center. Additional cell line information can be found in Supplementary Table 1.

BM or peripheral blood samples for *in vitro* studies were obtained from patients with AML or ALL. Samples were collected during routine diagnostic procedures after written informed consent was obtained; protocols for studies in humans were approved by the Human Subjects Committee of MD Anderson Cancer Center.

Mononuclear cells were separated by Ficoll-Hypaque (Sigma-Aldrich) density gradient centrifugation. Cell lines and primary samples were maintained in RPMI 1640 medium containing 10% fetal calf serum (Gemini Bio-Products) and 1% penicillin-streptomycin (Life Technologies Laboratories). Patient characteristics are shown in Supplementary Table S2.

Normoxic culture conditions comprised 21% O_2 and 5% CO_2 at 37°C. For experiments involving hypoxic conditions (1% O_2 and 5% CO_2 at 37°C) cells were incubated in the hypoxic Workstation INVIVO2 400 (Ruskinn Technology).

mRNA hybridization and gene-expression profiling by Nanostring technology

Total RNA was amplified and hybridized to Illumina HT12 version 4 human whole-genome arrays as described previously(28). For Nanostring analysis, mononuclear cells from BM and peripheral blood samples from patients with acute leukemia or healthy subjects were lysed to isolate total mRNA. For each sample, 100 ng of mRNA was used to set up Nanostring codeset 5; the genes included in the analysis are listed in Supplementary Table S3.

Magnetic Resonance Imaging

Imaging was performed on a 7-Tesla, 30-cm bore Biospec MR imaging system (Bruker Biospin Corp., Ettlingen, Germany) equipped with a Bruker gradient/shim system BGA-12 (200 mT/m maximum strength; 80 μs rise time). Prior to scanning, each mouse was anesthetized, catheterized via tail vein, and placed in the lateral decubitus position on a custom animal bed distributing 2% isoflurane in oxygen and circulating warm water. A linear, dual-tuned $^{1}H/^{13}C$ radio-frequency (RF) coil with 72-mm inner diameter was used for ^{1}H imaging and ^{13}C transmission. To enhance sensitivity and localize signal reception to the femur, a custom-built 15-mm ^{13}C receive-only surface coil was placed over the femur as shown in Figure 2A. Vital signs were carefully monitored throughout the experiments. The imaging protocol began with T_1-weighted positioning scans, followed by rapid gradient echo multi-plane scout localizers. High-resolution T_2-weighted sagittal and axial images were then acquired (echo time TE = 17 ms; repetition time TR = 2,500 ms; 156 × 156-μm in-plane resolution; 4-cm field-of-view; 10 2-mm slices; 4 averages), providing visualization of the femur and offering a means for subsequent ^{13}C slice prescription.

Hyperpolarized Magnetic Resonance Spectroscopy

To generate HP-pyruvate, a 26-mg sample of neat [1-^{13}C]pyruvic acid (Sigma-Aldrich), containing 15 mM of OX063 radical (GE Healthcare) and 1.5 mM Prohance (Bracco Diagnostics Inc.), was polarized in a HyperSense DNP system (Oxford Instruments) as previously described(29, 30). The frozen sample was rapidly dissolved, resulting in a final isotonic and neutral solution containing 80mM [1-^{13}C]pyruvate. Please refer to Supplemental Methods for further details.

In vitro TH-302 cytotoxicity assay

Cells were seeded at 1×10^{6} cells/mL, treated with TH-302 at a final concentration of 5, 7.5, 10, or 15 μM, and incubated in normoxic or hypoxic ($1\%O_2$) conditions for 6 h. The medium was then replaced with fresh medium to yield cell suspensions at 0.25×10^{6} cells/mL, and cells were incubated in normoxic conditions for 48h until collection for FACS analysis. For combination studies, cells were seeded at 0.2×10^{6}/mL, treated with the indicated drugs, and incubated under normoxic or hypoxic conditions for 48 or 72h. Combination index values were calculated by utilizing Calcusyn software (Biosoft, Cambridge, UK).

Cell viability assay

Following treatment, cells were washed twice in phosphate-buffered saline solution (PBS) and resuspended in 100 μL Annexin binding buffer containing Annexin V–Cy5 (BD Biosciences). After 15-min incubation in the dark, cells were washed and resuspended in Annexin binding buffer containing 7AAD or PI. Cells were quantitated after the addition of 10,000 CountBright counting beads (Invitrogen) per sample. Annexin V–positive cells were analyzed by a FACSCalibur flow cytometer (BD Biosciences) or a FACS Array Bioanalyzer (BD Biosciences), and results are presented as percentage of Annexin V–positive cells. In the case of primary human samples, results are expressed as percentage of specific apoptosis, calculated as: (% AnnV-positive cells in the sample – % AnnV-positive cells in the control)/(100 – %AnnV-positive cells in the control) × 100.

Murine tumor models

All animal work was done in accordance with a protocol approved by the Institutional Animal Care and Use Committee of MD Anderson Cancer Center. Please refer to Supplementary Methods for a detailed description of each model used.

Detection of hypoxia in BM

Following chemotherapy and TH-302 treatment, hypoxia probe pimonidazole (PIMO) was administered intraperitoneally at 100 mg/kg. Three hours later, mice were euthanized and their femurs and tibiae were processed for IHC.

Statistical analysis

Unless otherwise indicated, results are expressed as mean ± SEM of three independent experiments. *P*-values were determined by one-way ANOVA followed by F statistics or paired *t*-test (when comparing two groups). A *P*-value less than 0.05 was considered significant. Survival analysis for in vivo studies was done using Mantel-Cox and Gehan-Breslow-Wilcoxon tests. Unless otherwise noted, all calculations were carried out by the GraphPad Prism software (GraphPad) software.

Results

Hypoxia signature expression in leukemia cell lines and primary samples

We previously used chemical probes of hypoxia to detect expansion of hypoxic niches in murine leukemia-bearing BM(5), and additionally found stabilization of HIF-1α in BM from leukemia patients(9). To elucidate molecular changes associated with the hypoxic nature of the leukemic BM microenvironment, we first established a set of hypoxia-regulated genes in leukemia cells utilizing genome-wide gene expression profiling (GEP). To this end, total RNA from REH or OCI-AML3 human leukemia cell lines, each cultured for 48 h at 21% or 1% O_2 was used for GEP by microarrays. Using strict significance criteria (*P* value < 0.01, false discovery rate *q* statistic < 0.1) for three independent experiments, we found 21 genes consistently upregulated by hypoxia in both cell lines (Supplementary Table S3). From these genes, we selected a “hypoxia set” that included genes known to be regulated by HIF transcription factors and/or that overlap with established hypoxia signatures in solid

tumors(31-33). Next, we utilized Nanostring probes to compare the hypoxia-related gene expression in samples from leukemia patients (N = 15, Supplementary Table S2) and normal healthy donors (N=4). The expression of 9 of the 21 genes interrogated, including *LDHA*, *EGLN1*, *HIF1AN, ARNT* and *TGFB,* was individually significantly different between leukemia patient samples and controls (Fig. 1A). When expression levels of these 21 genes were averaged to generate a "hypoxia index," 14 leukemic samples individually exhibited significantly higher index values as compared to normal donors, and the average normalized index value for all 15 leukemic patients 443.5 ± 49.26 (mean expression ± SEM) was significantly different from that of normal donors (100 ± 17.30, $P<0.0001$, Fig. 1B). The difference in hypoxic signature expression persisted when the analysis was performed comparing peripheral blood or BM from leukemic and normal donors (data not shown), likely reflecting durability of gene expression changes preserved in circulating cells upon exiting hypoxic marrow microenvironment. Our results suggest that leukemic blasts exhibit a hypoxic gene expression profile correlating with the presence of hypoxia in the setting of advanced leukemia.

In vivo assessment of metabolism in the leukemic BM

Since hypoxia confers metabolic shift towards glycolysis, we determined the level of glycolysis occurring in diseased (AML1/ETO bearing mice) versus healthy mice using *in vivo* HP-MR. C57Bl/6 mice were transplanted with murine cells expressing the AML1/ETO fusion oncoprotein, mutant NRAS and GFP in a p53-null background(34). These mice develop AML very rapidly and, if untreated, die of the disease with a median survival time of 27 days. A ^{13}C surface coil was placed on the femur and thigh of the animal to detect resonance frequency signal from hyperpolarized [1-^{13}C]-pyruvate and HP [1-^{13}C]-lactate (Fig. 2B). The HP lactate signal lags arrival of the concentrated bolus of HP pyruvate, and reflects direct chemical conversion of HP pyruvate into lactate through interaction with the intracellular enzyme lactate dehydrogenase. Over time, both signals decay beyond the dynamic range of the measurement due to signal losses caused by excitation, relaxation of polarization to thermal equilibrium, and washout(29, 30). The area under the HP lactate curve, normalized to the area under both lactate and pyruvate, gives insight into the relative rate of exchange of the HP ^{13}C label from pyruvate to lactate. The normalized lactate value measured from thigh and femur was significantly lower in normal animals compared to those bearing AML (Fig. 2C; $P < 0.01$), indicating higher rates of glycolysis in the leukemic microenvironment *in vivo*.

In Vitro High Resolution Metabolic Nuclear Magnetic Resonance Analysis

To further explore the metabolic profile of pyruvic acid, *in vitro* AML/ETO cells were incubated in media containing 1 mM of 1-^{13}C pyruvic acid and compared to control (See Supplementary). Aliquots were taken at time of addition of the media (t_o), 1 hour into the incubation (t_1), and 8 hours into the incubation (t_8). All media aliquot samples were analyzed using one dimensional (1D) proton-decoupled ^{13}C NMR spectroscopy. The amount of 1-^{13}C pyruvate still remaining in the media after 1 and 8 hours into the incubation compared to the initial time point (t_0) was used to determine the percentage of pyruvate uptake. The values can be seen in Supplementary Table S4. Based on these values, approximately 11% of the pyruvate is taken up by the culture in 1 hour and increases to 89%

of pyruvate in 8 hours. Spectral resonances for lactate and pyruvate were not seen in control t_8 aliquots by ^{13}C NMR analysis. A resonance for lactate was observed only in t_1 and t_8 pyruvate aliquot samples. These observations confirm that AML/ETO can utilize pyruvate to generate lactic acid readily similar to what was observed in HP-MR *in vivo* studies.

Targeting hypoxia in vitro *with TH-302*

Given our findings indicating that hypoxia is a prevalent feature of the leukemic BM microenvironment, and because of the known role of hypoxia in tumor biology and chemoresistance, we studied targeting hypoxia in leukemia with the HAP TH-302.We first tested this agent's antitumor activity *in vitro* against several leukemic cell lines representing diverse acute leukemia subtypes, including KBM-5 (chronic myeloid leukemia), KG-1, OCI-AML3, MOLM-13 (AML), REH and Nalm-6 (pre-B-ALL). Fig. 3A shows dose-dependent cytotoxicity in the cell lines tested, summarized in Supplementary Table S5 by the median inhibitory concentrations (IC_{50}) for normoxia and hypoxia, and a hypoxia cytotoxicity ratio (HCR) reflecting the hypoxia-selective cell killing. Sensitivity varied across cell lines, but was consistently much greater in hypoxia. Nalm-6 cells were the most sensitive (IC_{50} in normoxia and hypoxia: 1.3 and 0.005μM, respectively). We extended our results to primary ALL (#1 and #2) and AML (#3) samples, which exhibited drug-dependent cytotoxicity under hypoxic but not normoxic conditions (Fig. 3B). Importantly, TH-302 was able to target the leukemic stem cell–enriched CD34+/CD123+ population in a primary AML sample, as shown in Fig. 3C. In contrast, TH-302 exhibited minimal cytotoxic activity against four normal bone marrow samples (Fig. 3D).

To better recapitulate the multidimensional BM niche, we next utilized co-cultures of green fluorescent protein (GFP)-labeled leukemic cells (OCI-AML3 or MOLM-13) with BM-derived red fluorescent protein (RFP)–labeled mesenchymal stromal cells (MSCs) immobilized within Matrigel to generate three-dimensional (3D) structures (spheroids). The cells within the spheroids co-proliferated over time with colonies of leukemic cells firmly attached to MSC, as shown by confocal microscopy (Supplementary Fig. 1). Extensive hypoxia was present in the MSC/AML spheroids grown at normal oxygen tension, as revealed by PIMO staining (Supplementary Fig. 2). We then determined the anti-leukemia activity of TH-302 in spheroid co-cultures of MSCs plus MOLM-13 or OCI-AML3 cells. TH-302 induced extensive apoptosis and reduced viability of leukemia cells by >60% in 3D spheroid co-cultures at 10-50 nM (Supplementary Fig. 1A, B).

The anti-leukemia efficacy of TH-302 was next tested in combination with chemotherapy agents frequently used for treatment of AML (cytarabine, doxorubicin) or with demethylating agents 5-azacytidine or decitabine (Supplementary Fig. 3). Combinations of TH-302 with cytarabine or with decitabine were synergistic or additive in killing OCI-AML3 and MOLM-13 AML cells under hypoxic conditions (average combination index values 0.69 and 0.67 for cytarabine plus TH-302 in MOLM-13 and OCI-AML3, respectively; 0.09 and 1.1 for doxorubicin plus TH-301 in MOLM-13 and OCI-AML3, respectively; 0.3 and 0.5 for decitabine or 5-azacytidine plus TH-302 in OCI-AML3, respectively).

In vivo anti-leukemia activity of TH-302

To validate our *in vitro* observations, we tested the anti-leukemia efficacy of TH-302 in models of AML *in vivo*. NOD/Scid/IL2Rγ-KO mice (NSG) transplanted with a primary AML sample were treated with vehicle or TH-302 after the presence of circulating human CD45+ cells (∼5%) was confirmed by FACS (Day 37). TH-302 (administered by intraperitoneal injection at 50 mg/kg 3 times a week for 3 weeks) prolonged survival of AML-bearing mice compared to the vehicle-treated mice (Fig. 4A; median survival time: TH-302 = 75 days; Control = 56 days; P = 0.003, n = 8 mice/group) and reduced the number of circulating AML cells by week 3 (2-3 mice were characterized: controls, 17.3 and 9.2×10^6 cells/mL, respectively; TH-302, 2.3, 5.5, and 0.53×10^6 cells/mL, respectively; Fig. 4B). PIMO staining revealed substantial reduction of the hypoxic areas in the BM of treated mice compared to control mice (Fig. 4C). To test the ability of HAPs to target leukemia-initiating cells, secondary transplant experiments were performed in which BM cells from control or TH-302–treated mice, collected after 2 weeks of therapy, were injected into secondary NSG recipient mice at 1×10^4 cells/mouse (N = 5 mice). At the time of secondary transplants, both control and TH-302-treated mice had high (>70% CD45+ cells in the bone marrow) leukemia burden, despite reduction of the total white blood count. Although all transplanted mice died from leukemia, survival of animals injected with cells from TH-302–treated primary recipients was prolonged compared to that of vehicle-treated controls (median survival of mice transplanted with cells from recipients, 68 days; and of mice transplanted with cells from primary recipients treated with TH-302, 79 days; $P = 0.003$; Fig. 4D). This was accompanied by delayed detection of circulating huCD45+ cells in mice transplanted with cells from TH-302–treated mice, while huCD45+ cells were detectable in control mice by week 4 after transplantation (Supplementary Fig. 4).

We next tested the antitumor efficacy of TH-302 and the multikinase inhibitor sorafenib in the aggressive MOLM-13 FLT3/ITD *in vivo* model. Sorafenib and TH-302 synergistically decreased viability and induced apoptosis in MOLM-13 cells *in vitro*, particularly under hypoxic conditions (CI value = 0.055, Supplementary Fig. 5). Starting on day 3 after transplantation of MOLM-13-LUC cells, NSG mice were treated with TH-302 or sorafenib, alone or in combination, for 2 weeks. Disease progression was monitored by optical bioluminescence imaging (BLI). The combination of TH-302 and sorafenib had the greatest effect in prolonging mouse survival compared to vehicle treatment (p= 0.0009), but each drug alone also prolonged survival, with TH-302 proving to be more effective than sorafenib alone (mean survival time: controls, 17.8 days; TH-302, 28.3 days; sorafenib, 24.6 days; combination, 32 days; Fig. 5A). The anti-leukemia effects were also evidenced by reduced bioluminescence imaging intensity in the treated groups than in the vehicle-treated animals (Fig. 5B, C).

AML cells surviving chemotherapy remain hypoxic and can be targeted by TH-302 leading to survival extension

Based on recent evidence suggesting that cancer stem cells reside in hypoxic niches that protect them from chemotherapeutics and are responsible for disease recurrence after treatment(2, 35, 36), we determined whether hypoxia was still present after disease debulking using the AML1/ETO syngeneic leukemia model. On day 18 after transplantation

when engraftment was confirmed by detection of circulating GFP+ cells by FACS, mice were randomized and treated with vehicle or chemotherapy (cytarabine plus doxorubicin, DA) for 5 days. Treatment was effective in reducing circulating GFP-positive cells (controls, 11.5 ± 4.9, N = 6; treatment, 0.52 ± 0.27, N=8; Fig. 6A), mimicking the disease in humans. To determine the persistence of hypoxia, mice were administered the hypoxia marker PIMO one week after completion of AD chemotherapy and sacrificed. Immunohistochemical staining of the BM from these mice revealed that while hypoxia was greatly expanded in control mice with high leukemia burden, it persisted in residual cells surviving chemotherapy (Fig. 6B).

Based on the evidence that the leukemic niches remain hypoxic after chemotherapy, we tested whether targeting residual hypoxic leukemic cells with TH-302 had any beneficial anti-leukemia effect. At one week post chemotherapy treatment, when only minimal residual bone marrow infiltration was detectable by BLI, mice were randomized to receive vehicle or TH-302 for the next 2 weeks. While chemotherapy reduced tumor burden and extended survival, administration of TH-302 in the setting of residual disease further prolonged survival, with a few mice surviving more than 50 days (mean survival duration: vehicle, 27 days; chemotherapy plus vehicle, 36 days; chemotherapy plus TH-302, 42 days; P = 0.0002; Fig. 6C, D). To examine the effects of TH-302 on hypoxic leukemic cells in the bone marrow, we performed an independent experiment in which AML/ETO-transplanted mice received vehicle, DA chemotherapy or TH-302 for 5 days. We next compared the fraction of PIMO-binding AML cells in control mice, mice treated with DA or TH-302, following PIMO injection and immunohistochemical staining. As reported by us previously, healthy mice did not show PIMO positivity in the bone marrow, consistent with lack of gross hypoxia (Supplemental Figure 6A top panel). In turn, extended areas of PIMO binding were detectable in both, control and DA-treated animals, while selective reduction of hypoxic areas was seen in TH-302 treated mice (Supplemental Figures 6A, B).

Discussion

The results shown in this work highlight hypoxia's role as a major feature of the microenvironment. Gene expression profiling of peripheral blood and BM samples from healthy donors and patients with leukemia demonstrated that patients with leukemia have greater “hypoxia signature” expression than controls. The fact that this difference was identifiable even in peripheral blood suggests that the expansion of the hypoxic niche that we and others have described as a common phenomenon of acute BM disease translates into long-lasting gene expression changes in cells that are influenced by the microenvironment. Among the genes that were differentially expressed were the two negative regulators of HIF-1α:*EGLN1* and *HIFAN;* and genes involved in glycolytic metabolism *LDHA and PGK1*. In agreement with our findings, Rapin *et al.*, recently reported common transcriptional programs in AML patients that included a striking upregulation of the hypoxic response gene signature(37). These transcriptome changes can lead to, or reflect, metabolic reprogramming of cells. A clear link between hypoxia and glycolysis has been established, whereby hypoxia-induced HIF-1α promotes the expression of several enzymes involved in glycolytic pathways(12, 38, 39). *In vivo* metabolic imaging of the BM has proven to be challenging because of technical and anatomical limitations. However,

development of noninvasive hyperpolarized ^{13}C MR, providing 10,000-fold signal amplification over conventional MR, made possible interrogation of the *in vivo* glycolytic metabolic status of the BM(29, 40, 41). Utilizing HP-^{13}C pyruvate, we found a higher glycolytic rate in murine leukemic BM compared to healthy marrow, as indicated by the greater conversion of pyruvate to lactate. We have preliminary data that the pyruvate conversion to lactate could be occurring primarily in the stromal cells compared to the AML/ETO cells (data not shown). This is consistent with recent publications indicating that increased glycolysis could be caused by stromal cells in close proximity to cancer cells and that there is metabolic crosstalk between the two cell types(42-45). This finding provides yet another piece of evidence supporting the metabolic re-programming of BM niches as a consequence of reduced oxygen availability in diseased BM.

The mechanism for hypoxia development in the leukemic BM remains elusive. Our working hypothesis is that leukemic blasts are intrinsically hypoxic because their high rate of proliferation depletes oxygen rapidly. Although not addressed in the present work, it has been speculated that a defective vasculature in the diseased BM might also contribute to generation of a hypoxic niche. Indeed, Schaefer *et al.* reported that the microvasculature in a murine AML model was heterogeneous, resembling the defective angiogenesis observed in solid tumors and associated with disease progression(46). The role of hypoxia in promoting resistance to chemotherapy and stemness and increasing tumor invasiveness has been widely studied, and our published work together with current findings support the presence of hypoxia in the leukemic BM microenvironment and provide a strong rationale for exploiting hypoxia as a therapeutic target.

Hypoxic cells can be targeted by inhibiting HIFs that are required for survival of hypoxic cells(47-49). Very recently, both HIF-1 and HIF-2 have been implicated in the maintenance of leukemia-initiating cells(50, 51), but these transcription factors remain challenging drug targets, with no selective inhibitors available in clinical practice. An alternative approach is to use hypoxia-activated prodrugs that selectively target hypoxic cells. Several HAPs have advanced to clinical testing, mainly in solid tumors but more recently also in hematological malignancies(25). The hypoxia-selective activity of TH-302 has been demonstrated in a wide range of tumor cell lines, including a multiple myeloma *in vivo* model(27). It is not known what genetic characteristics underlie cell line-specific differences in sensitivity or resistance to TH-302 in vitro. This same broad range of cytotoxic potency (over two logs) was observed by Meng et al. across 32 cell lines(26) and more recently in the Hunter et al. 2014 study in triple-negative breast cancer cell lines (>∼30× range of cytotoxicity).(52) Several factors have been identified that can underlie differences in sensitivity to TH-302 in vitro: (1) variations in the expression levels of the one-electron reductases necessary for the activation of the prodrug; (2) differences in the activity of the specific DNA damage response and repair pathways in response to TH-302; and (3) differences in cell fate as a consequence of the DNA damage (e.g. cell cycle arrest, cell death). Currently in clinical development, HAP TH-302 is being tested for a broad series of indications including AML/ALL. Preliminary results of a Phase I clinical trial of single-agent TH-302 in patients with advanced leukemia (n = 34) have been reported, with transient responses suggesting clinical activity(53).

Here we showed that TH-302 had impressive hypoxia-dependent activity in several leukemia cell lines and primary patient samples and in a 3D system developed to resemble the leukemic niche *in vitro*. Recent work by Portwood *et al*. demonstrated that TH-302 induced double-stranded DNA breaks, cell cycle arrest, and ultimately cell death in *in vitro* models of AML under hypoxic conditions(54). Our findings expand on this work by demonstrating *in vivo* activity of TH-302 in several other AML xenograft models. Most importantly, we found that administration of TH-302 a week after chemotherapy treatment to mice with minimal residual disease prolonged survival, suggesting that this approach may be suitable for eliminating chemotherapy-resistant leukemia-initiating cells. In addition, we determined that residual leukemic BM cells in a syngeneic AML model remain hypoxic after chemotherapy; and that TH-302 selectively reduces hypoxia in AML marrows. We also demonstrated that TH-302 has synergistic and additive effects in combination with conventional chemotherapy and demethylating agents *in vitro*, as has been observed in preclinical solid tumor models(55). In line with the *in vitro* data, we also showed that TH-302 has potent activity in combination with sorafenib in the aggressive MOLM-13 FLT3/ITD *in vivo* model. The data included in Figure 3D indicate only minor toxicity against normal hematopoietic cells. Yet, we believe that one can expect some degree of myelosupression as on-target side effect of HAPs, which could be in particular apparent in combinations with other cytotoxic agents. In clinical trials with TH-302 moderate myelosuppression was observed but this did not constitute dose limiting toxicity (DLT). When TH-302 was combined with other myelosuppressive agents as part of a combination regimen in the clinical trials (e.g. TH-302 plus doxorubicin for soft tissue sarcoma) more myelosuppression was observed than what could be expected with doxorubicin alone, but this was not dose limiting.(56)

In summary, the work presented here extends our understanding of the hypoxic nature of the leukemic BM microenvironment. Our *in vivo* and *in vitro* metabolic data offer hints on the metabolic rewiring occurring in the diseased marrow and provide additional “metabolic” therapeutic targets. We showed that HAPs can be utilized effectively to target leukemic cells and hypoxic leukemia-initiating cells and that combination of HAPs with chemotherapy and/or other targeted therapies may constitute a successful therapeutic regimen for patients with acute leukemia.

Supplementary Material

Refer to Web version on PubMed Central for supplementary material.

Acknowledgments

The authors thank Dr. Scott W Lowe (Cold Spring Harbor) for kindly providing the AML1/ETO cells.

Grant Support: This research was supported in part by Threshold Pharm., Leukemia and Lymphoma Scholar in Clinical Research 2189-12 (to M. Konopleva), the National Institutes of Health 5 R01 CA155056-03 (to M. Konopleva), Leukemia Spore 5 P50 CA100632-08 DRP award (to M. Konopleva), Cancer Center Support Grant P30CA016672 and the Cancer Prevention and Research Institute of Texas RP101243-P5. This research was supported in part by Leukemia SPORE Developmental Award NCI P50 CA100632 (to P. Bhattacharya), MD Anderson Institutional Research Grant (to N.Z. Millward) and R21 CA 185536-01 (to P. Bhattacharya and N.Z. Millward), CDMRP PC110065 (to N.Z. Millward) and NCI Cancer Center Grant CA016672 for the support of the NMR Facility at MD Anderson Cancer Center.

Reference List

1. Estey EH. Acute myeloid leukemia: 2013 update on risk-stratification and management. Am J Hematol. 2013; 88:318–27. [PubMed: 23526416]
2. Konopleva MY, Jordan CT. Leukemia stem cells and microenvironment: biology and therapeutic targeting. JClinOncol. 2011; 29:591–9.
3. Azab AK, Hu J, Quang P, Azab F, Pitsillides C, Awwad R, et al. Hypoxia promotes dissemination of multiple myeloma through acquisition of endothelial to mesenchymal transition-like features. Blood. 2012
4. Storti P, Bolzoni M, Donofrio G, Airoldi I, Guasco D, Toscani D, et al. Hypoxia-inducible factor (HIF)-1alpha suppression in myeloma cells blocks tumoral growth in vivo inhibiting angiogenesis and bone destruction. Leukemia. 2013
5. Liu H, Diaz-Flores E, Poire X, Koval G, Malnassy G, Le Beau MM, et al. Targeting multiple signal pathways simultaneously might provide effective therapeutic strategies in acute myeloid leukemia. J Clin Oncol. 2011; 29
6. Pouyssegur J, Dayan F, Mazure NM. Hypoxia signalling in cancer and approaches to enforce tumour regression. Nature. 2006; 441:437–43. [PubMed: 16724055]
7. Schioppa T, Uranchimeg B, Saccani A, Biswas SK, Doni A, Rapisarda A, et al. Regulation of the chemokine receptor CXCR4 by hypoxia. J Exp Med. 2003; 198:1391–402. [PubMed: 14597738]
8. Semenza GL. Targeting HIF-1 for cancer therapy. Nat Rev Cancer. 2003; 3:721–32. [PubMed: 13130303]
9. Frolova O, Samudio I, Benito JM, Jacamo R, Kornblau SM, Markovic A, et al. Regulation of HIF-1alpha signaling and chemoresistance in acute lymphocytic leukemia under hypoxic conditions of the bone marrow microenvironment. Cancer Biol Ther. 2012; 13:858–70. [PubMed: 22785211]
10. Konoplev S, Kornblau SM, Schlette E, Lu H, Thomas DA, Zhang N, et al. Overexpression of HIF1 Alpha Predicts Worse Overall and Event-Free Survival in Patients with Philadelphia Chromosome-Negative Precursor B-Lymphoblastic Leukemia. Blood. 2008; 112:870–1.
11. Matsunaga T, Imataki O, Torii E, Kameda T, Shide K, Shimoda H, et al. Elevated HIF-1alpha expression of acute myelogenous leukemia stem cells in the endosteal hypoxic zone may be a cause of minimal residual disease in bone marrow after chemotherapy. Leuk Res. 2012; 36:e122–4. [PubMed: 22444690]
12. Marin-Hernandez A, Gallardo-Perez JC, Ralph SJ, Rodriguez-Enriquez S, Moreno-Sanchez R. HIF-1alpha modulates energy metabolism in cancer cells by inducing over-expression of specific glycolytic isoforms. Mini Rev Med Chem. 2009; 9:1084–101. [PubMed: 19689405]
13. Mimeault M, Batra SK. Hypoxia-inducing factors as master regulators of stemness properties and altered metabolism of cancer- and metastasis-initiating cells. J Cell Mol Med. 2013; 17:30–54. [PubMed: 23301832]
14. Griffin JL. Metabonomics: NMR spectroscopy and pattern recognition analysis of body fluids and tissues for characterisation of xenobiotic toxicity and disease diagnosis. Current opinion in chemical biology. 2003; 7:648–54. [PubMed: 14580571]
15. Beckonert O, Keun HC, Ebbels TM, Bundy J, Holmes E, Lindon JC, et al. Metabolic profiling, metabolomic and metabonomic procedures for NMR spectroscopy of urine, plasma, serum and tissue extracts. Nature protocols. 2007; 2:2692–703. [PubMed: 18007604]
16. Golman K, Zandt RI, Lerche M, Pehrson R, Ardenkjaer-Larsen JH. Metabolic imaging by hyperpolarized 13C magnetic resonance imaging for in vivo tumor diagnosis. Cancer Res. 2006; 66:10855–60. [PubMed: 17108122]
17. Brindle KM, Bohndiek SE, Gallagher FA, Kettunen MI. Tumor imaging using hyperpolarized 13C magnetic resonance spectroscopy. Magn Reson Med. 2011; 66:505–19. [PubMed: 21661043]
18. Nelson SJ, Kurhanewicz J, Vigneron DB, Larson PE, Harzstark AL, Ferrone M, et al. Metabolic imaging of patients with prostate cancer using hyperpolarized [1-(1)(3)C]pyruvate. Science translational medicine. 2013; 5:198ra08.
19. Guise CP, Wang AT, Theil A, Bridewell DJ, Wilson WR, Patterson AV. Identification of human reductases that activate the dinitrobenzamide mustard prodrug PR-104A: A role for NADPH :

cytochrome P450 oxidoreductase under hypoxia. Biochemical Pharmacology. 2007; 74:810–20. [PubMed: 17645874]

20. Wang J, Foehrenbacher A, Su J, Patel R, Hay MP, Hicks KO, et al. The 2-nitroimidazole EF5 is a biomarker for oxidoreductases that activate bioreductive prodrug CEN-209 under hypoxia. Clin Cancer Res. 2012; 18:1684–95. [PubMed: 22167409]
21. Guise CP, Abbattista MR, Tipparaju SR, Lambie NK, Su J, Li D, et al. Diflavin oxidoreductases activate the Bioreductive Prodrug PR-104A under Hypoxia. Mol Pharmacol. 2012; 81:31–40. [PubMed: 21984255]
22. Mason RP, Holtzman JL. The role of catalytic superoxide formation in the O2 inhibition of nitroreductase. BiochemBiophysResCommun. 1975; 67:1267–74.
23. Benito J, Shi Y, Szymanska B, Carol H, Boehm I, Lu H, et al. Pronounced hypoxia in models of murine and human leukemia: high efficacy of hypoxia-activated prodrug PR-104. PLoSONE. 2011; 6:e23108.
24. Konopleva M, Thall PF, Arana YiC, Borthakur G, Coveler A, Bueso-Ramos C, et al. Phase I/II study of the hypoxia-activated prodrug PR104 in refractory/relapsed acute myeloid leukemia and acute lymphoblastic leukemia. Haematologica. 2015
25. Benito J, Zeng Z, Konopleva M, Wilson WR. Targeting hypoxia in the leukemia microenvironment. International journal of hematologic oncology. 2013; 2:279–88. [PubMed: 24490034]
26. Meng F, Evans JW, Bhupathi D, Banica M, Lan L, Lorente G, et al. Molecular and cellular pharmacology of the hypoxia-activated prodrug TH-302. Mol Cancer Ther. 2012; 11:740–51. [PubMed: 22147748]
27. Hu J, Handisides DR, Van VE, De RH, Menu E, Vande BI, et al. Targeting the multiple myeloma hypoxic niche with TH-302, a hypoxia-activated prodrug. Blood. 2010; 116:1524–7. [PubMed: 20530289]
28. Jacamo R, Chen Y, Wang Z, Ma W, Zhang M, Spaeth EL, et al. Reciprocal leukemia-stroma VCAM-1/VLA-4-dependent activation of NF-kappaB mediates chemoresistance BH3 profiling discriminates response to cytarabine-based treatment of acute myelogenous leukemia HDAC inhibition by SNDX-275 (Entinostat) restores expression of silenced leukemia-associated transcription factors Nur77 and Nor1 and of key pro-apoptotic proteins in AML. Blood. 2014; 123:2691–702. [PubMed: 24599548]
29. Ardenkjaer-Larsen JH, Fridlund B, Gram A, Hansson G, Hansson L, Lerche MH, et al. Increase in signal-to-noise ratio of > 10,000 times in liquid-state NMR. Proc Natl Acad Sci U S A. 2003; 100:10158–63. [PubMed: 12930897]
30. Sandulache VC, Skinner HD, Wang Y, Chen Y, Dodge CT, Ow TJ, et al. Glycolytic inhibition alters anaplastic thyroid carcinoma tumor metabolism and improves response to conventional chemotherapy and radiation. Mol Cancer Ther. 2012; 11:1373–80. [PubMed: 22572813]
31. Khong TL, Thairu N, Larsen H, Dawson PM, Kiriakidis S, Paleolog EM. Identification of the angiogenic gene signature induced by EGF and hypoxia in colorectal cancer. BMC Cancer. 2013; 13:518. [PubMed: 24180698]
32. Srivastava M, Khurana P, Sugadev R. Lung cancer signature biomarkers: tissue specific semantic similarity based clustering of digital differential display (DDD) data. BMC research notes. 2012; 5:617. [PubMed: 23122428]
33. Eustace A, Mani N, Span PN, Irlam JJ, Taylor J, Betts GN, et al. A 26-gene hypoxia signature predicts benefit from hypoxia-modifying therapy in laryngeal cancer but not bladder cancer. Clin Cancer Res. 2013; 19:4879–88. [PubMed: 23820108]
34. Zuber J, Radtke I, Pardee TS, Zhao Z, Rappaport AR, Luo W, et al. Mouse models of human AML accurately predict chemotherapy response. Genes Dev. 2009; 23:877–89. [PubMed: 19339691]
35. Keith B, Simon MC. Hypoxia-inducible factors, stem cells, and cancer. Cell. 2007; 129:465–72. [PubMed: 17482542]
36. Takubo K, Suda T. Roles of the hypoxia response system in hematopoietic and leukemic stem cells. Int J Hematol. 2012; 95:478–83. [PubMed: 22539363]

37. Rapin N, Bagger FO, Jendholm J, Mora-Jensen H, Krogh A, Kohlmann A, et al. Comparing cancer vs normal gene expression profiles identifies new disease entities and common transcriptional programs in AML patients. Blood. 2014; 123:894–904. [PubMed: 24363398]
38. Kim JW, Tchernyshyov I, Semenza GL, Dang CV. HIF-1-mediated expression of pyruvate dehydrogenase kinase: a metabolic switch required for cellular adaptation to hypoxia. Cell metabolism. 2006; 3:177–85. [PubMed: 16517405]
39. Semenza GL. HIF-1 mediates metabolic responses to intratumoral hypoxia and oncogenic mutations. J Clin Invest. 2013; 123:3664–71. [PubMed: 23999440]
40. Golman K, Zandt R, Thaning M. Real-time metabolic imaging. Proc Natl Acad Sci U S A. 2006; 103:11270–5. [PubMed: 16837573]
41. Bohndiek SE, Kettunen MI, Hu DE, Kennedy BW, Boren J, Gallagher FA, et al. Hyperpolarized [1-13C]-ascorbic and dehydroascorbic acid: vitamin C as a probe for imaging redox status in vivo. J Am Chem Soc. 2011; 133:11795–801. [PubMed: 21692446]
42. Lisanti MP, Martinez-Outschoorn UE, Chiavarina B, Pavlides S, Whitaker-Menezes D, Tsirigos A, et al. Understanding the “lethal” drivers of tumor-stroma co-evolution: emerging role(s) for hypoxia, oxidative stress and autophagy/mitophagy in the tumor micro-environment. Cancer Biol Ther. 2010; 10:537–42. [PubMed: 20861671]
43. Samudio I, Fiegl M, McQueen T, Clise-Dwyer K, Andreeff M. The warburg effect in leukemia-stroma cocultures is mediated by mitochondrial uncoupling associated with uncoupling protein 2 activation. Cancer Res. 2008; 68:5198–205. [PubMed: 18593920]
44. Morandi A, Chiarugi P. Metabolic implication of tumor:stroma crosstalk in breast cancer. J Mol Med (Berl). 2014; 92:117–26. [PubMed: 24458539]
45. Fiaschi T, Marini A, Giannoni E, Taddei ML, Gandellini P, De Donatis A, et al. Reciprocal metabolic reprogramming through lactate shuttle coordinately influences tumor-stroma interplay. Cancer Res. 2012; 72:5130–40. [PubMed: 22850421]
46. Schaefer C, Krause M, Fuhrhop I, Schroeder M, Algenstaedt P, Fiedler W, et al. Time-course-dependent microvascular alterations in a model of myeloid leukemia in vivo. Leukemia. 2008; 22:59–65. [PubMed: 17898789]
47. Nordgren IK, Tavassoli A. Targeting tumour angiogenesis with small molecule inhibitors of hypoxia inducible factor. Chem Soc Rev. 2011; 40:4307–17. [PubMed: 21483947]
48. Xia Y, Choi HK, Lee K. Recent advances in hypoxia-inducible factor (HIF)-1 inhibitors. Eur J Med Chem. 2012; 49:24–40. [PubMed: 22305612]
49. Onnis B, Rapisarda A, Melillo G. Development of HIF-1 inhibitors for cancer therapy. J Cell Mol Med. 2009; 13:2780–6. [PubMed: 19674190]
50. Wang Y, Liu Y, Malek SN, Zheng P. Targeting HIF1alpha eliminates cancer stem cells in hematological malignancies. Cell Stem Cell. 2011; 8:399–411. [PubMed: 21474104]
51. Rouault-Pierre K, Lopez-Onieva L, Foster K, Anjos-Afonso F, Lamrissi-Garcia I, Serrano-Sanchez M, et al. HIF-2alpha protects human hematopoietic stem/progenitors and acute myeloid leukemic cells from apoptosis induced by endoplasmic reticulum stress. Cell Stem Cell. 2013; 13:549–63. [PubMed: 24095676]
52. Hunter FW, Hsu HL, Su J, Pullen SM, Wilson WR, Wang J. Dual targeting of hypoxia and homologous recombination repair dysfunction in triple-negative breast cancer. Mol Cancer Ther. 2014; 13:2501–14. [PubMed: 25193512]
53. Konopleva M, Handisides D, Lorente GA, Benito JM, Borthakur G, Jabbour E, Faderl S, Cortes JE, Kroll S, Andreeff M, Kantarjian H, Thomas DA. A Phase 1 Study of TH-302, a Hypoxia-Activated Cytotoxic Prodrug, in Subjects with Advanced Leukemias. ASCO 2012 Annual Meeting. 2012
54. Portwood S, Lal D, Hsu YC, Vargas R, Johnson MK, Wetzler M, et al. Activity of the hypoxia-activated prodrug, TH-302, in preclinical human acute myeloid leukemia models. Clin Cancer Res. 2013; 19:6506–19. [PubMed: 24088735]
55. Liu Q, Sun JD, Wang J, Ahluwalia D, Baker AF, Cranmer LD, et al. TH-302, a hypoxia-activated prodrug with broad in vivo preclinical combination therapy efficacy: optimization of dosing regimens and schedules. Cancer ChemotherPharmacol. 2012; 69:1487–98.

56. Chawla SP, Cranmer LD, Van Tine BA, Reed DR, Okuno SH, Butrynski JE, et al. Phase II study of the safety and antitumor activity of the hypoxia-activated prodrug TH-302 in combination with doxorubicin in patients with advanced soft tissue sarcoma. J Clin Oncol. 2014; 32:3299–306. [PubMed: 25185097]

Translational Relevance

The prognosis for AML remains poor indicating the urgent clinical need for better therapies. While targeting hypoxia in cancer has been proposed over 30 years ago, our data indicate that hypoxia is an essential component of the leukemic bone marrow microenvironment. This study demonstrates that targeting cells residing in hypoxic niches is feasible and may render leukemic cells drug sensitive. Utilization of hypoxia-activated prodrugs such as TH-302 should be considered to tackle the microenvironmental chemoresistance in leukemia therapy.

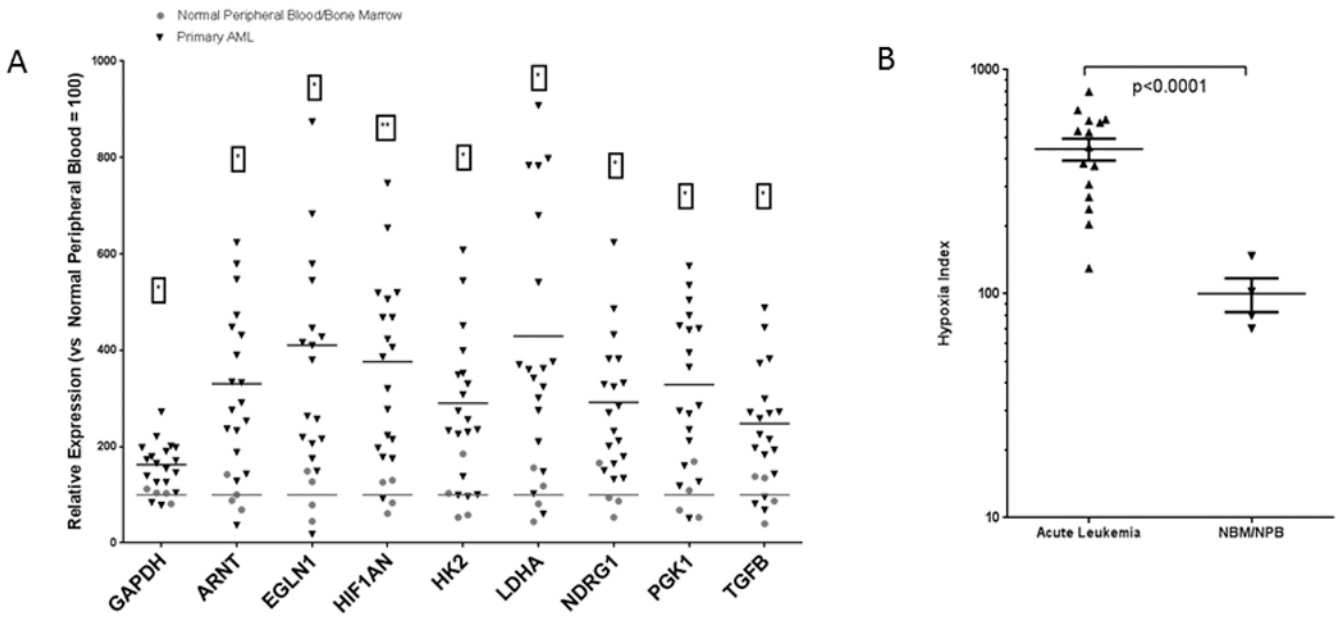

Figure 1. Leukemic blasts express a "hypoxia signature"

Bone marrow (BM, n=3) and peripheral blood (PB, n=12) samples from patients with AML (N=15) and healthy subjects (PB n=2, BM n=2) were collected during routine diagnostic procedures and subjected to Nanostring analysis. A. Genes whose expression in AML samples was significantly different than that in normal samples. B. Hypoxia signature index (calculated for each sample by averaging the relative expression of all genes with detectable levels) in samples from healthy donors and patients with AML. P-value was calculated using unpaired t-test with Welch's correction.

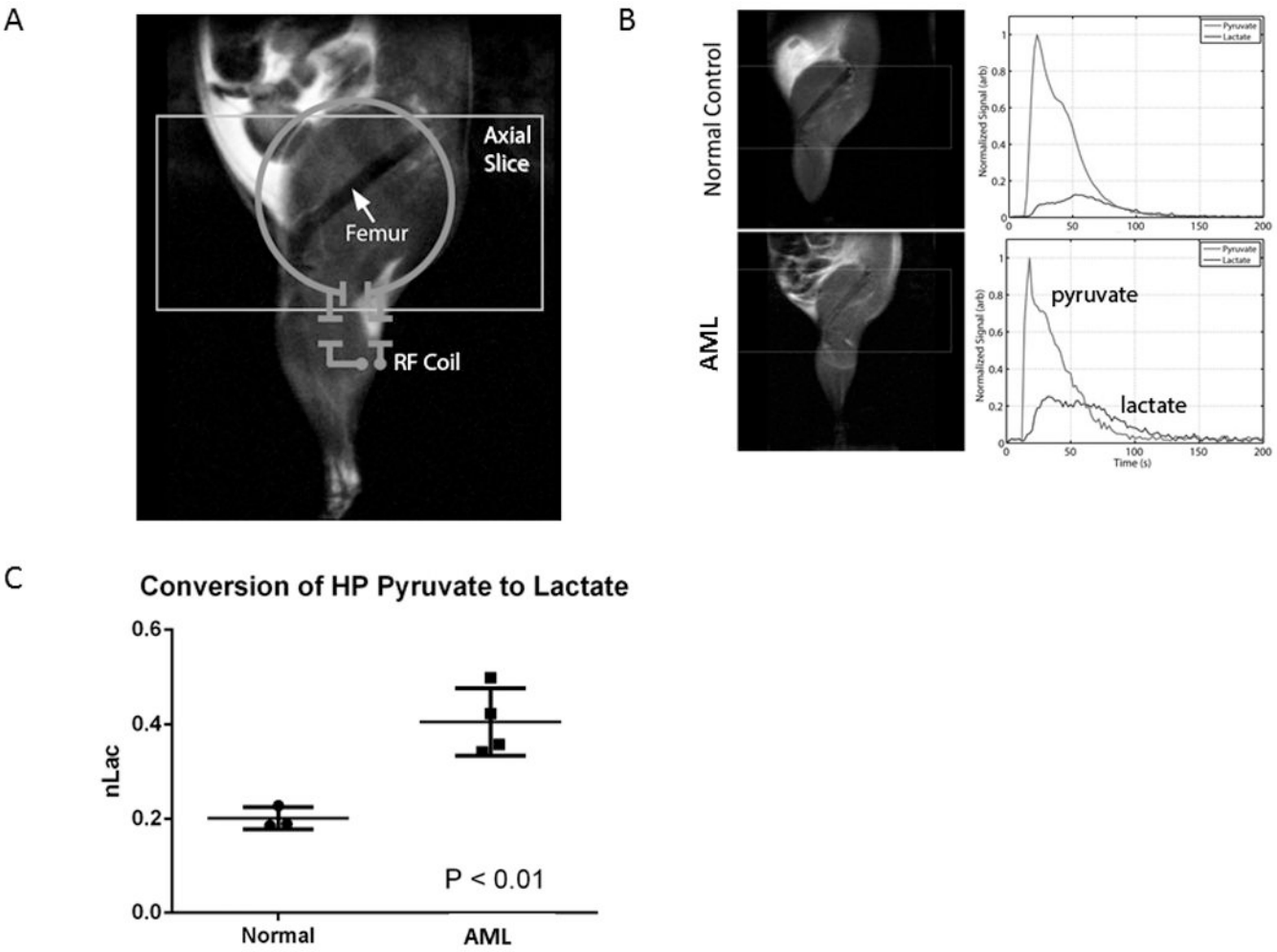

Figure 2. Metabolic hyperpolarized-pyruvate NMR reveals differences between normal and AML murine bone marrow

A. Illustration of slice prescription and RF coil placement for hyperpolarized (HP) ^{13}C acquisitions. B. (Left) T_2-weighted anatomic images of normal control (top) and AML-bearing animal (bottom). (Right) Representative traces illustrate the arrival of HP pyruvate and its subsequent conversion into HP lactate. C. Normalized area under the HP lactate curve (nLac), which corresponds with the rate of conversion of the bolus of pyruvate into lactate.

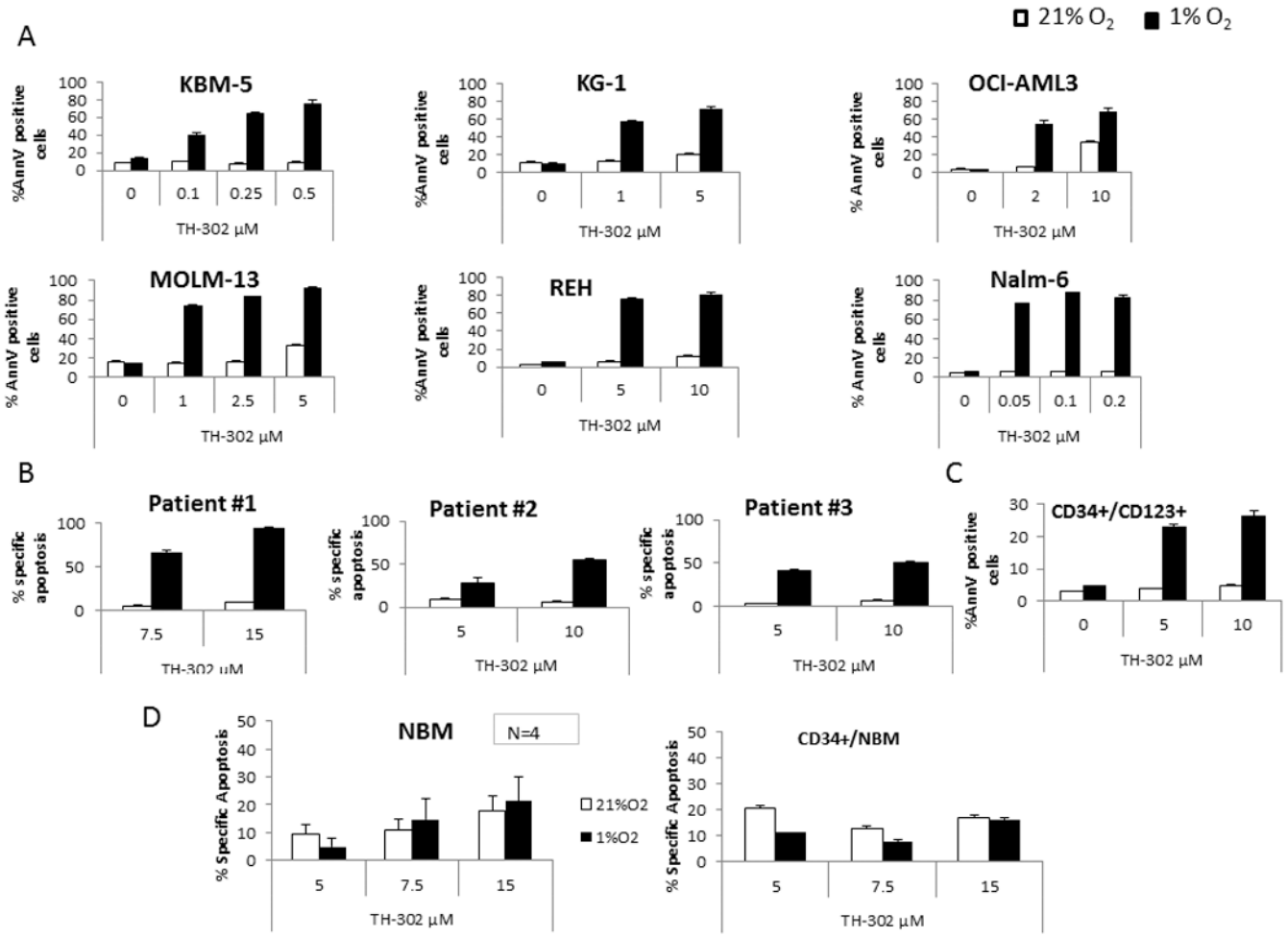

Figure 3. TH-302 has hypoxia-selective cytotoxicity against leukemia cell lines and primary AML samples

A. KBM-5, KG-1, OCI-AML3, MOLM-13, REH, and Nalm-6 cells were exposed to the indicated doses of TH-302 for 6 h under normoxic (21% O_2, white bars) or hypoxic (1% O_2, black bars) conditions and then were washed and incubated for 48 h under normoxic conditions. Effects on apoptosis induction were determined by FACS. B. Three primary leukemia samples (samples #1 and 2 are from ALL patients, sample #3 is from an AML patient) were treated as indicated in A and then were allowed to recover for 24 h under normoxic conditions before cell death was assessed by FACS. C. For patient #3, effect of TH-302 was also determined on the leukemia stem cell–enriched compartment (CD34+/CD123+ cells). D. In vitro cytotoxic activity of TH-302 against normal bone marrow cells. MNC from normal BM samples were exposed to TH-302 as indicated for the primary leukemic samples. Effects on apoptosis induction on the whole population (N=4) or the CD34+ (N=1) cells were determined by FACS (mean of 3 repeats; error bars=SEM).

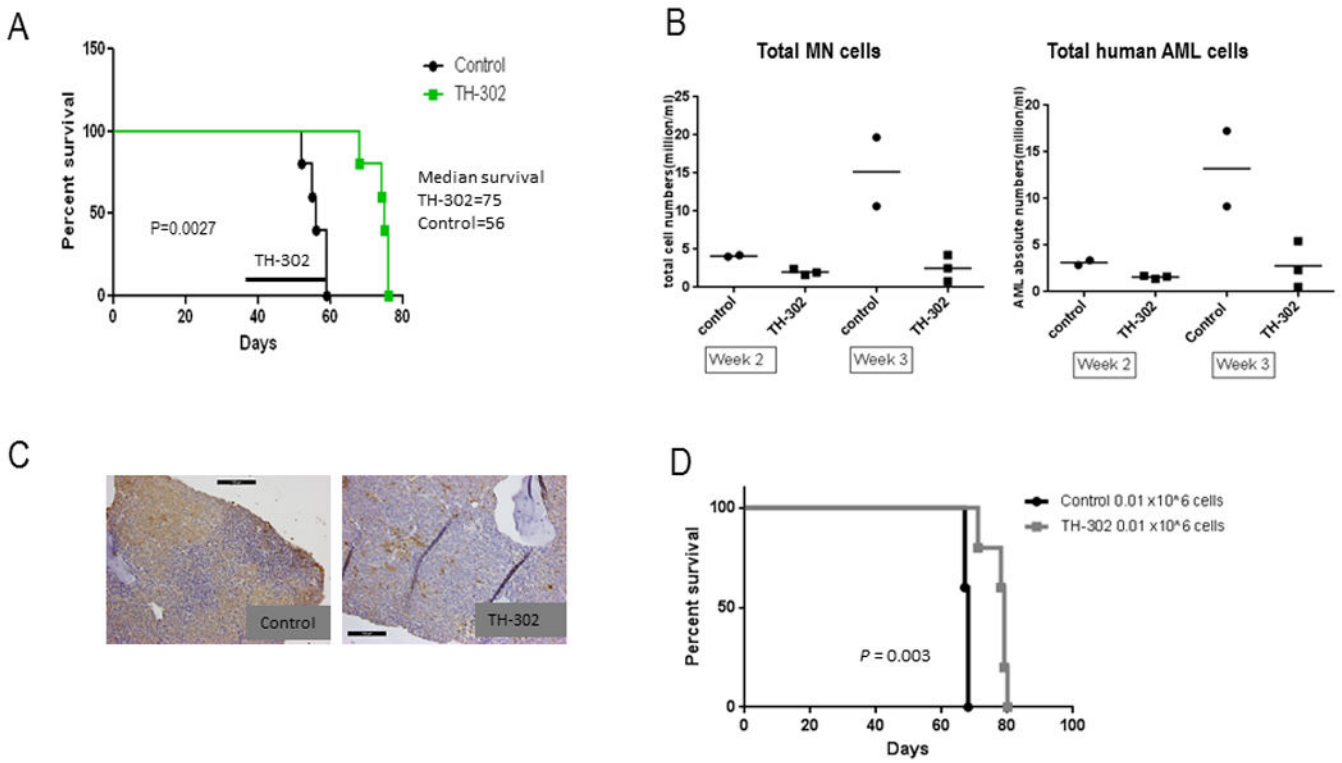

Figure 4. TH-302 has anti-leukemia activity in an *in vivo* primary AML xenograft murine model

TH-302 (50 mg/kg intraperitoneally 3 times a week for 3 weeks) reduced the number of circulating AML cells and prolonged survival of NSG mice engrafted with primary AML cells compared to the vehicle-treated mice. A. Survival curves (N=8/group) of vehicle-treated (control) and TH-302–treated mice. Line indicates onset and duration of treatment. B. Total numbers of mononuclear cells (MN) or total human AML cells were determined in blood by FACS analysis after staining for huCD45 (N=2 and 3 for control and TH-302–treated mice, respectively). C. PIMO immunostaining of BM sections from control or TH-302–treated mice euthanized at the end of the treatment; 20 × magnification. D. Survival curves of secondary transplant mice (N=5/group). NSG mice were transplanted with 0.01 or 0.005×10^6 BM cells isolated from primary recipients (A) treated with control or TH-302. * $P<0.05$; ** $P<0.01$; *** $P<0.001$.

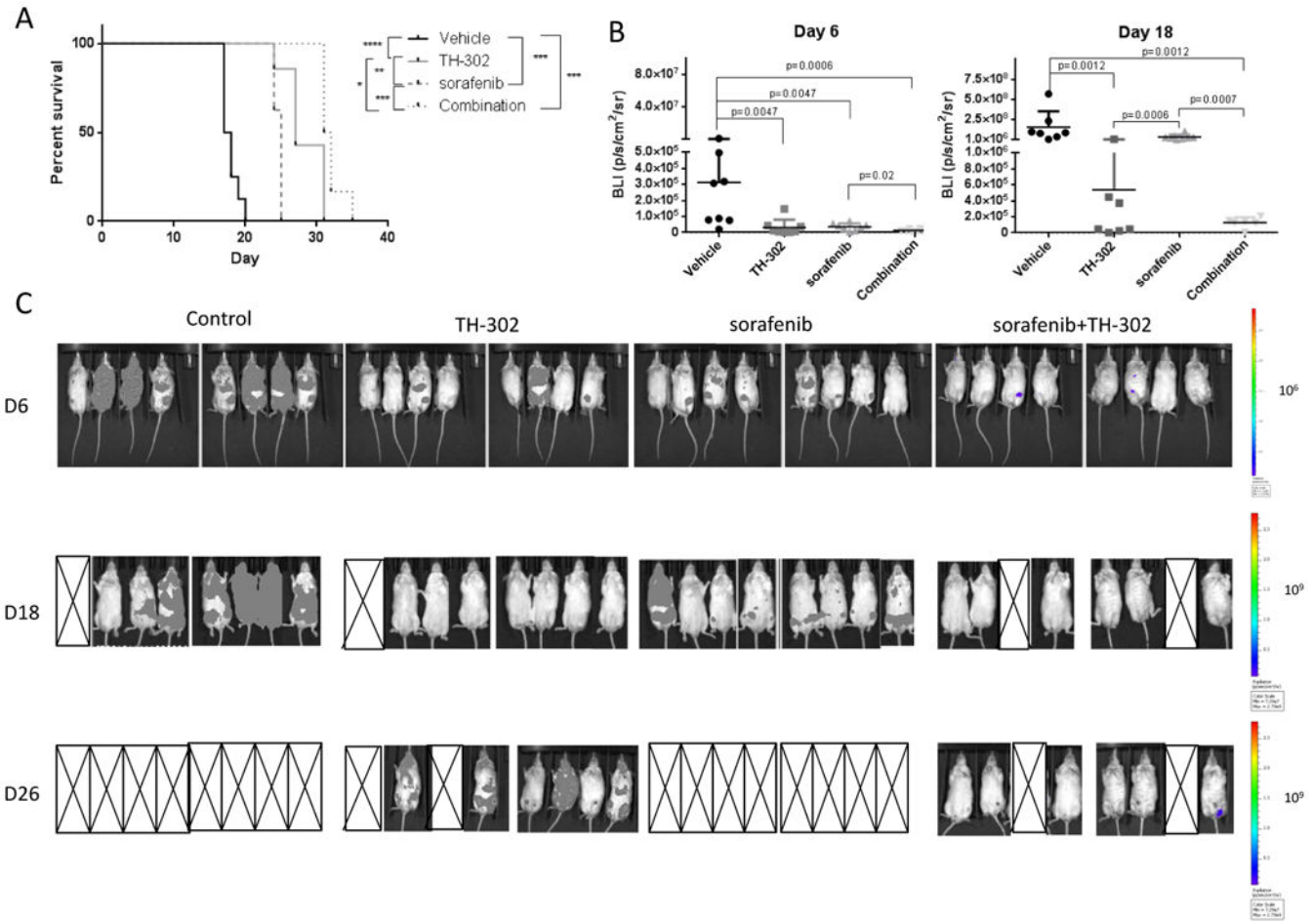

Figure 5. TH-302 and sorafenib have synergistic activity *in vivo*

A. Survival curves of NSG mice (N=5/group) transplanted with FLT/3ITD MOLM-13-LUC-GFP cells and treated with TH-302, sorafenib, or a combination starting on day 3 after cell injection. B. Quantification of tumor burden from bioluminescence images (BLI) on day 6 and 18 after cell transplantation. C. Optical imaging of mice transplanted with MOLM-13 cells and treated with vehicle, TH-302, sorafenib or the combination of TH-302 and sorafenib and performed on days 6, 18 and 26 after transplantation. X denotes mice that died.* $P<0.05$; ** $P<0.01$; *** $P<0.001$.

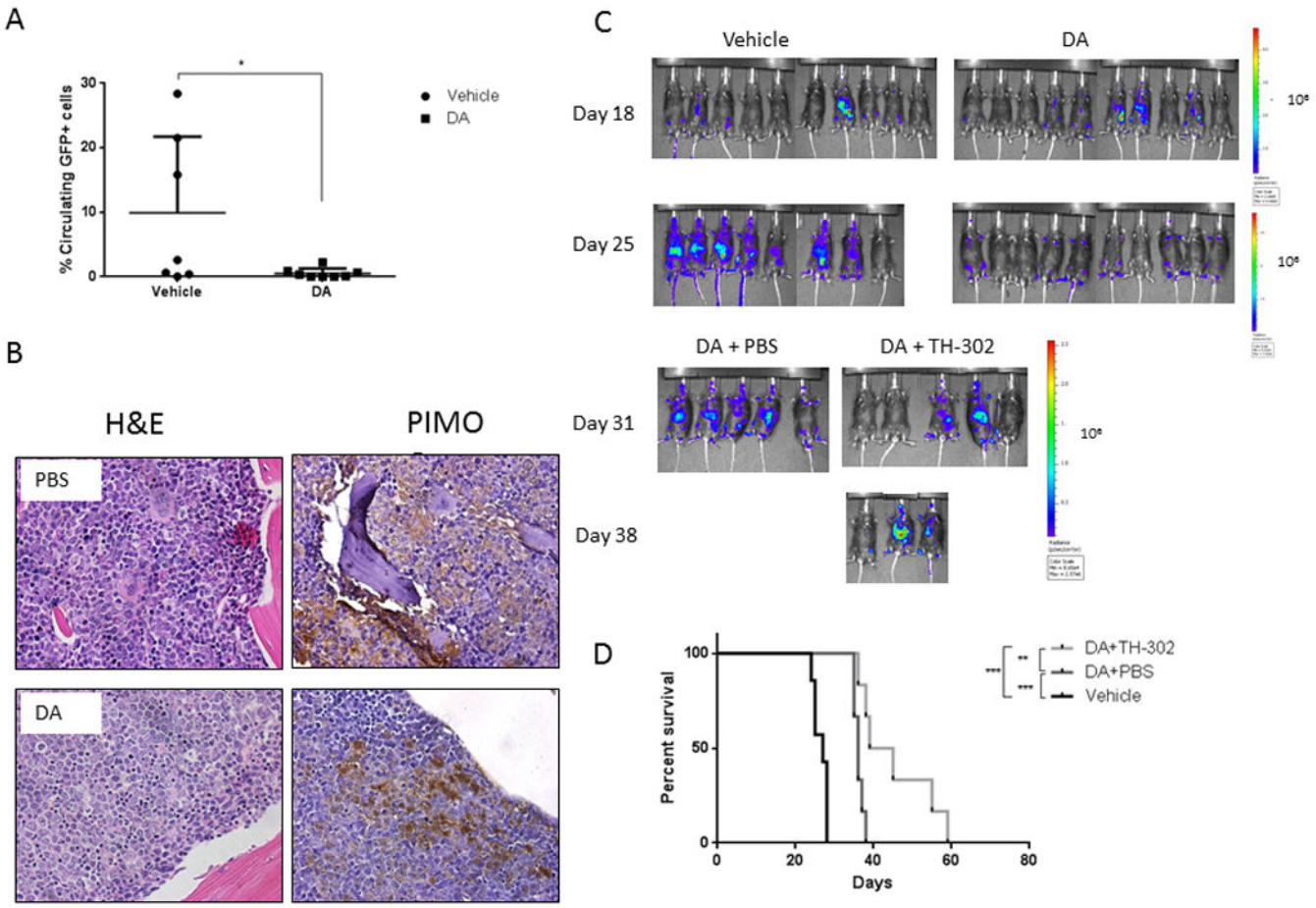

Figure 6. TH-302 administration after chemotherapy improves survival in a syngeneic AML murine model

C57Bl/6 mice were injected with AML1/ETO-GFP cells and treated with doxorubicin and cytarabine (DA). A. Percentage of circulating GFP-positive cells at the end of chemotherapy. B. Pimonidazole (PIMO) immunostaining reveals persistence of hypoxia in the leukemic BM post-chemotherapy. Shown are PIMO and hematoxylin and eosin (H&E) staining of BM from control (PBS) and treated mice that were euthanized 1 week after completing the treatment and 3 h after receiving PIMO. C. Optical density images of C57Bl/6 mice transplanted with AML1/ETO-LUC-GFP cells and treated with vehicle (PBS) or chemotherapy for 5 days; after 1 week of recovery, mice were treated with TH-302. D. Survival curves of mice treated as described in C (N=6/group). * $P<0.05$; ** $P<0.01$; *** $P<0.001$.